

## Pulmonary Retention of Adipose Stromal Cells Following Intravenous Delivery Is Markedly Altered in the Presence of ARDS

Hongyan Lu,\*†‡§ Todd Cook,\*†‡ Christophe Poirier,¶ Stephanie Merfeld-Clauss,\*†‡§ Irina Petrache,†‡§¶ Keith L. March,\*†‡§ and Natalia V. Bogatcheva\*†‡§

\*Division of Cardiology, Indiana University, Indianapolis, IN, USA

†Indiana Center for Vascular Biology and Medicine, Indiana University, Indianapolis, IN, USA

‡VC-CAST Signature Center, Indiana University, Purdue University, Indianapolis, IN, USA

§Roudebush Veteran Affairs Medical Center, Indianapolis, IN, USA

¶Division of Pulmonary and Critical Care Medicine, Indiana University, Indianapolis, IN, USA

Transplantation of mesenchymal stromal cells (MSCs) has been shown to effectively prevent lung injury in several preclinical models of acute respiratory distress syndrome (ARDS). Since MSC therapy is tested in clinical trials for ARDS, there is an increased need to define the dynamics of cell trafficking and organ-specific accumulation. We examined how the presence of ARDS changes retention and organ-specific distribution of intravenously delivered MSCs isolated from subcutaneous adipose tissue [adipose-derived stem cells (ADSCs)]. This type of cell therapy was previously shown to ameliorate ARDS pathology. ARDS was triggered by lipopolysaccharide (LPS) aspiration, 4 h after which 300,000 murine CRE<sup>+</sup> ADSCs were delivered intravenously. The distribution of ADSCs in the lungs and other organs was assessed by real-time polymerase chain reaction (PCR) of genomic DNA. As anticipated, the majority of delivered ADSCs accumulated in the lungs of both control and LPS-challenged mice, with minor amounts distributed to the liver, kidney, spleen, heart, and brain. Interestingly, within 2 h following ADSC administration, LPS-challenged lungs retained significantly lower levels of ADSCs compared to control lungs (~7% vs. 15% of the original dose, respectively), whereas the liver, kidney, spleen, and brain of ARDS-affected animals retained significantly higher numbers of ADSCs compared to control animals. In contrast, 48 h later, only LPS-challenged lungs continued to retain ADSCs (~3% of the original dose), whereas the lungs of control animals and nonpulmonary organs in either control or ARDS mice had no detectable levels of ADSCs. Our data suggest that the pulmonary microenvironment during ARDS may lessen the pulmonary capillary occlusion by MSCs immediately following cell delivery while facilitating pulmonary retention of the cells.

**Key words:** Acute respiratory distress syndrome (ARDS); Adipose-derived stem cells (ADSCs); Transplantation; Retention

### INTRODUCTION

Acute respiratory distress syndrome (ARDS) is a devastating critical condition where lungs fail to oxygenate blood due to a massive inflammatory response. ARDS patients require ventilation and face 40% mortality in cases of severe ARDS<sup>1</sup>. Even with substantial progress reached with improvement of supportive care, the need for lung-protective therapy is hard to overestimate<sup>2</sup>. While pharmacological therapies tested so far have not been successful in reducing mortality<sup>3,4</sup>, in the last decade preclinical studies have shown strong promise for mesenchymal stem cells (MSCs), including those derived from adipose tissue (ADSCs)<sup>5,6</sup>.

MSC transplantation via intravenous (IV) delivery is a minimally invasive procedure; however, it is associated

with a certain risk of pulmonary capillary bed occlusion and thromboembolism<sup>7</sup>. As patients with ARDS are already at higher risk for thromboemboli<sup>8</sup>, assessment of lung-specific accumulation of transplanted cells and dynamics of their retention in lungs and other organs are of utmost importance.

To trace transplanted cells, researchers label them with fluorophores, such as radioactive or nuclear magnetic resonance (NMR) probes. While detection of conventional fluorescent probes presents problems of autofluorescence, photobleaching, and short penetration depth<sup>9</sup>, more advanced probes such as infrared quantum dots (QDs)<sup>10</sup>, and probes for positron emission tomography (PET) and magnetic resonance imaging (MRI)<sup>11</sup> require specialized equipment to assess the labeled cell distribution. To overcome this

Received September 24, 2015; final acceptance June 2, 2016. Online prepub date: November 25, 2015.

Address correspondence to Natalia V. Bogatcheva, Ph.D., ICVBM, 1481 W 10th Street, C3105, Indianapolis, IN 46202, USA. Tel: (317) 988-4535; Fax: (317) 988-9325; E-mail: [nbogatch@iu.edu](mailto:nbogatch@iu.edu)

problem, we utilized adipose-derived stem cells (ADSCs) isolated from genetically modified mice carrying CRE expression under a Tie2 promoter<sup>12</sup>. As the Tie2 promoter is not specific for ADSCs, detection is possible by analysis of genomic DNA with CRE-specific primers.

Lungs seem to be privileged organs when it comes to the retention of IV-delivered particles<sup>11,13</sup>, as it represents the first capillary bed met by the particles delivered to the peripheral vein. Not surprisingly, the first clinical trials using MSCs (NCT01775774 at clinicaltrials.gov) and ADSCs<sup>14</sup> for treatment of ARDS intravenously administered the cells. However, one possible complication of IV delivery is pulmonary capillary bed occlusion and thromboembolism of the lung<sup>7</sup>; therefore, the dosage and the speed of delivery, along with the vasoconstrictive status of the patient, should be taken into account.

In the current study, we determined the ability of naive and lipopolysaccharide (LPS)-primed lungs (and other organs) to retain IV-delivered ADSCs. This study had three objectives: (1) to determine if ADSC retention in lungs is increased in ARDS; (2) to determine the length of ADSC retention in ARDS lungs; and (3) to determine if ADSCs are redistributed to other organs. To understand ARDS-specific dynamics of cell distribution, we analyzed cardiac output and parameters indicative of pulmonary pressure in LPS-challenged mice. The results of our study are informative of the safety of IV ADSC therapy for ARDS and the dynamics of ADSC retention in lungs for future therapy optimization.

## MATERIALS AND METHODS

### Materials

*Escherichia coli* LPS 0127:B8 with the lot activity of 3,000,000 U/mg and fluorescein isothiocyanate (FITC)-dextran (40 kDa) were purchased from Sigma-Aldrich (St. Louis, MO, USA).

### Animals

Twelve-week-old female C57BL/6 mice were purchased from Harlan Laboratories (Indianapolis, IN, USA). Tie2 CreERT2 mice were generously provided by Dr. Carlesso from Indiana University. Transgenic mice on the original background<sup>12</sup> received from Dr. Carlesso (Indiana University) had been bred with C57BL/6 for two generations, and then the strain was maintained as a closed colony by breeding transgenic males with nontransgenic females from the same colony. All animal procedures were approved by the Indiana University Institutional Animal Care and Use Committee (IACUC) and conformed to the requirements of the Animal Welfare Act.

### Cell Culture

Murine ADSCs (mADSCs) were isolated from subcutaneous fat pads of female heterozygous Tie2CreERT2

carriers (3–4 months old). Briefly, fat was excised from the isoflurane-anesthetized animals ( $n=3$ ), minced, and digested with 2 mg/ml collagenase type 1 (Worthington Biochemical, Lakewood, NJ, USA) at 37°C. Digested tissue was centrifuged at 300×g to separate floating adipocytes. Pellets containing the stromal vascular fraction were resuspended in Endothelial Basal Medium-2 (EBM2; Lonza, Basel, Switzerland) with 5% fetal bovine serum (FBS; Lonza), filtered through a 100-μm nylon filter, and centrifuged again at 300×g. Cells were resuspended in Endothelial Growth Medium EGM2-MV (Lonza), allowed to adhere to plastic, and propagated until the third passage (P3) at 37°C in a humidified atmosphere of 5% CO<sub>2</sub> and 95% O<sub>2</sub>. Before injection, cells were trypsinized (Lonza) and resuspended in EBM2 at a concentration of 3 × 10<sup>6</sup> cells/ml.

### Cell Tracing Experiment

LPS (2 mg/kg) or an equal volume of saline was delivered by oropharyngeal aspiration to isoflurane-anesthetized C57BL/6 mice (20–25 g) as previously described<sup>15</sup>. Control mice received an equal volume of saline. ADSCs derived from Tie2CreERT2 mice<sup>12</sup> (P3) were resuspended at 3 × 10<sup>6</sup> cell/ml in EBM2 containing 6.25 mg/ml FITC-dextran, and injected into the tail vein (300,000 cells per mouse) 4 h after LPS administration. To ascertain the efficiency of cell injection, 10 min after injection blood was sampled from the saphenous vein and analyzed for FITC fluorescence. Animals anesthetized with isoflurane were exsanguinated; lung, heart, spleen, kidney, brain, and liver were collected immediately after cell injection, or 2, 24, or 48 h later ( $n=4$  for each time group). Organs were snap frozen in liquid nitrogen. Minced organs were subjected to complete digestion with enzymes from a mini total RNA kit for tissue (IBI Scientific, Peosta, IA, USA), and genomic DNA free of mRNA was extracted. DNA was analyzed with quantitative real-time polymerase chain reaction (qRT-PCR) for the presence of CRE transgene, using D19Mit1 as a loading control. The following primers were used: CRE, 5'-GCGGTCTGGCAGTAAAACTATC-3' and 5'-GTGAAACAGCATTTGCTGTCACTT-3'; D19Mit1: 5'-AATCCTTGTTCACTCTATCAAGGC-3' and 5'-CATGAAGAGTCCAGTAGAAACCTC-3'.

To establish that there was no tissue-specific interference with the qPCR reaction, calibration curves were created for DNA from each organ of interest isolated directly from Tie2CreERT2 animals. The quantity of CRE<sup>+</sup> cells per organ was calculated on the basis of the knowledge that the mouse cell contains 5.6 pg DNA/cell, and using the difference in C<sub>t</sub> to calculate the difference in the content of CRE<sup>+</sup> genomic DNA between organs from Tie2CreERT2 heterozygous animals and organs from C57BL/6 mice injected with cells from Tie2CreERT2 heterozygous animals. To enable calculation of the amount of CRE<sup>+</sup> cells

per the amount of DNA loaded into the PCR machine to the amount of CRE<sup>+</sup> cells per organ, we first established conditions assuring that total DNA digestion and extraction were achieved from each analyzed organ aliquot. Each organ was weighed and minced; two aliquots of minced tissue from each organ were weighed and fully digested to extract genomic DNA. DNA yield per organ was calculated. For the analysis of CRE<sup>+</sup> cells in lungs, 25 ng of extracted DNA was analyzed by StepOnePlus Real-Time PCR (Applied Biosystems, Foster City, CA, USA); for the rest of the organs, 500 ng was loaded to increase the sensitivity of detection. Each DNA sample was analyzed with CRE-specific and D19Mit1-specific primers; each PCR analysis included DNA from the specific CRE<sup>+</sup> organ. To equalize values generated in parallel PCR runs, we normalized the  $C_{t(\text{cre organ})}$  value as  $C_{t(\text{cre organ})} \times C_{t(\text{cre+})} / C_{t(\text{D19 organ+})}$ . To calculate the amount of CRE<sup>+</sup> cells per loaded amount of DNA, we divided total expected amount of cells (for example, 500 ng is expected to contain DNA from 89,286 cells) by  $2^{[\text{norm}C_{t(\text{cre organ})} - C_{t(\text{cre+})}]}$ . To arrive at the total number of cells per organ, we back calculated the amount of cells per loaded DNA sample to the total DNA yield per organ.

#### Echocardiography

It was recently shown that a parameter known as ratio between pulmonary acceleration time and ejection time (PAT/PET) is negatively correlated with right ventricle systolic pressure (RVSP)<sup>16</sup>. While RVSP measurement is an invasive procedure, PAT/PET can be easily assessed by echocardiography. Transthoracic closed-chest echocardiography was performed in isoflurane-anesthetized animals using 40-MHz solid-state transducers (Vevo 2100; VisualSonics, Toronto, ON, Canada). Two-dimensional images of pulmonary infundibulum and pulsed wave Doppler recordings of the pulmonary blood flow were obtained from the long axis view; the left ventricle was imaged from a short axis view. Color Doppler was used to visualize the highest area of flow in the pulmonary artery (PA); the pulsed wave Doppler was collected at this

location. Measurements of PAT and PET were performed offline. PAT was calculated as time from the onset of pulmonary flow to peak velocity by pulsed wave Doppler recording. PET was calculated as the time interval between the onset and the end of the systolic flow velocity. Cardiac output was calculated as a difference between the systolic and diastolic volume of the left ventricle, multiplied by the heart rate ( $n=3$  was for control and LPS-treated groups).

#### Statistical Analysis

Quantitative data are presented as mean  $\pm$  standard error of the mean (SEM). Statistical analysis was performed by *t*-test and *t*-test with Welch's correction (unequal variance) using Origin 8.0 (OriginLab, Northampton, MA, USA) or GraphPad Prism6 (GraphPad Software, San Diego, CA, USA) software. A value of  $p < 0.05$  was considered statistically significant.

## RESULTS

#### Study Design

Previously, we have shown that mice subjected to oropharyngeal LPS aspiration manifest severe hypothermic reactions 4 h after LPS administration<sup>17</sup>. That point was chosen as a "seek care" point to administer ADSC therapy. The current study was designed on the basis of our previous scheme of therapeutic delivery in order to understand the dynamics of ADSC retention in control mice and mice affected by LPS-induced lung injury. As presented in Figure 1, LPS or saline was delivered into the lungs through oropharyngeal aspiration. Intravenous ADSC injections were performed 4 h after LPS delivery. Since injections into the murine tail vein are often associated with incomplete transfer of injected material, we had to implement control over the efficiency of cell transfer. To achieve that, ADSCs were delivered in the media containing FITC-dextran. Sampling of blood from the saphenous vein 10 min after ADSC delivery allowed us to assess plasma fluorescence and exclude from analysis tissues from mice with plasma



**Figure 1.** Timeline of the in vivo study design. Times at which mice were sacrificed and tissues collected for analysis are shown with black rectangles.

fluorescence levels less than 70% of the mean plasma fluorescence level.

#### Retention of IV-Delivered ADSCs in Lungs and Other Organs

To analyze distribution of ADSCs in different organs of naive and LPS-challenged mice, we traced ADSCs isolated from genetically modified mice carrying a CRE transgene. Use of CRE<sup>+</sup> ADSCs gave us an opportunity to detect cells by the analysis of genomic DNA from the organ of interest. Comparison of titration curves for CRE transgene with titration curves for D19Mit1 marker (MGI ID: 91215, one locus per genome) revealed the presence of  $\geq 10$  loci of CRE transgene in the genome of the donor transgenic mice (Fig. 2A–C), which significantly

improved our ability to detect CRE<sup>+</sup> cells in organs with limited CRE<sup>+</sup> cell distribution.

Analysis of lungs from ADSC-injected mice receiving saline showed that approximately 10–15% of the 300,000 injected cells were retained in lungs for at least 2 h following cell injection. This amount was markedly reduced in the next 24 h, and levels became negligible at 48 h postinjection (Fig. 3A). On the contrary, LPS-challenged lungs retained significantly fewer cells immediately after injection (less than 3% of injected dose). This level was increased to  $\sim 7\%$  within the next 2 h, remained stable for the following 24 h, and was still substantial ( $\sim 3\%$ ) 48 h postinjection. Analysis of the spleen, liver, kidneys, brain, and heart demonstrated minor cell retention compared to the lung (Fig 3). We did not detect evidence of CRE<sup>+</sup> cell

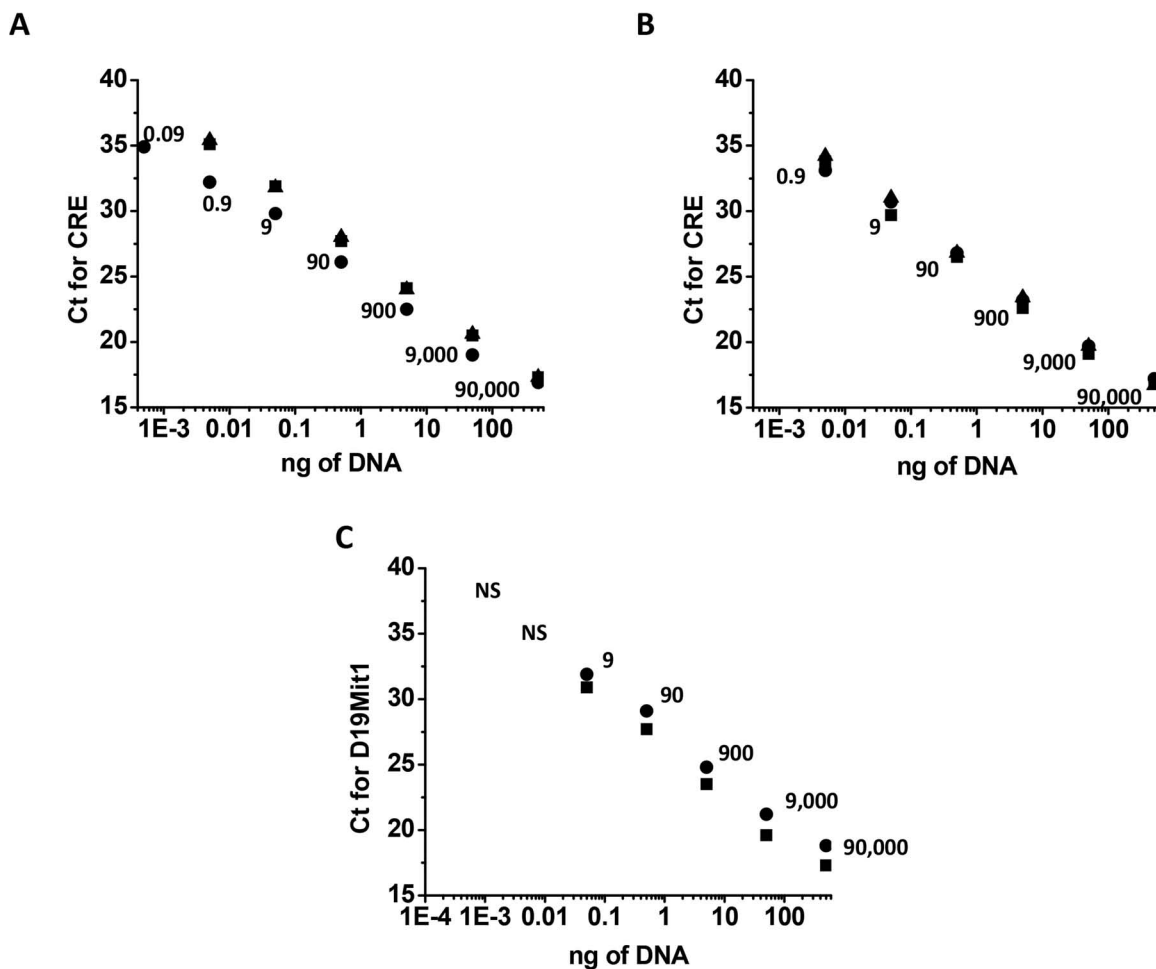


**Figure 2.** Real-time polymerase chain reaction (PCR) serial dilution standard curves for CRE transgene and D19Mit1 marker. Standard curves were constructed with CRE-specific primers for the serial dilutions of genomic DNA from the (A) lung (squares), spleen (circles), and heart (triangles), and (B) kidney (squares), liver (circles), and brain (triangles). (C) Parallel standard curves were constructed with D19Mit1-specific primers for lung (squares) and spleen (circles). DNA (500 ng) was loaded at the lowest dilution point. Estimated cell number for each dilution is shown on the plot. CRE is detected at higher dilution rates than D19Mit1 (one locus per genome), suggesting incorporation of multiple CRE copies at multiple loci. NS stands for not significant level of detection.

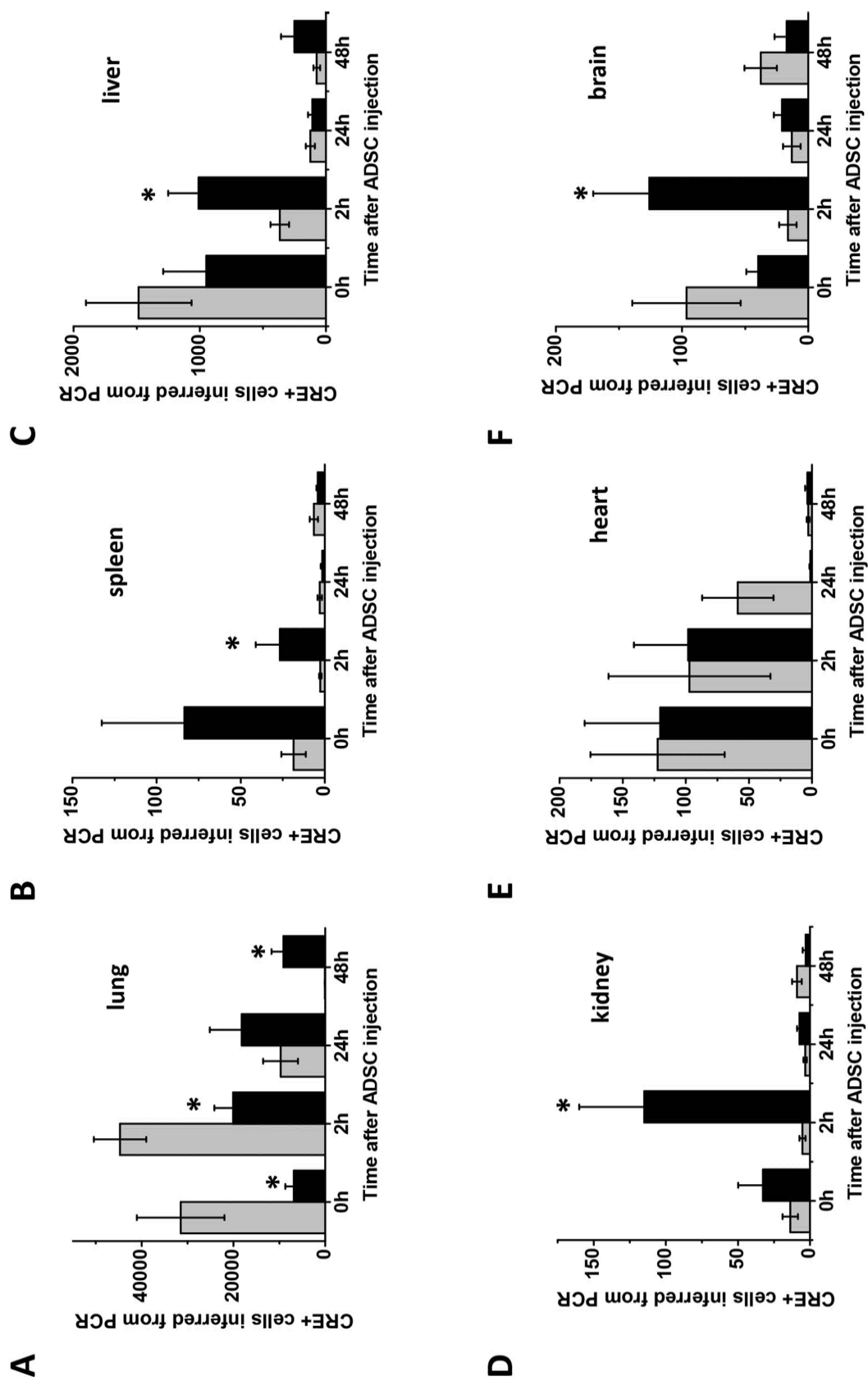


**Figure 3.** Distribution of intravenously delivered mADSCs in the lungs (A), spleen (B), liver (C), kidney (D), heart (E), and brain (F) of control (gray bars) and LPS-challenged (black bars) mice. Four mice were analyzed at each time point. Cell numbers were inferred from the real-time PCR data as explained in Materials and Methods. Lungs retained the majority of IV-delivered cells compared to other analyzed organs. LPS-primed lungs showed a lesser degree of cell retention immediately after injection and a greater amount of cells 48 h later. \* $p < 0.05$  between cell retention in organs of control animals and animals exposed to LPS.

translocation from the lung to other organs in the period between 24 and 48 h, when the level of CRE<sup>+</sup> cells in the lungs was significantly decreased. Interestingly, the majority of analyzed organs show control/LPS cell ratio opposite to the one observed in the lung 2 h postinjection. CRE<sup>+</sup> cell content in the spleen, liver, kidney, and brain of mice challenged with LPS was higher than that in organs of control mice. Importantly, 48 h postinjection, the only organ still showing significant CRE<sup>+</sup> cell retention was the LPS-challenged lung.

#### Assessment of Hemodynamics in ARDS Mice

To understand why LPS-primed lungs retain fewer ADSCs immediately following ADSC administration and 2 h later, we assessed parameters related to pulmonary pressure and cardiac output. Figure 4A shows that mice subjected to LPS aspiration experienced severe reductions

of PAT/PET 4 h after LPS administration, indicative of an increase in pulmonary pressure. We have also observed that 4 h after LPS administration, mice manifest marked reductions in heart rate (Fig. 4B). Although significant changes in stroke volume were not observed until 24 h after LPS administration (Fig. 4C), reduction in heart rate leads to a significant reduction of cardiac output 4 h after LPS administration (Fig. 4D).

#### DISCUSSION

This is the first study to demonstrate that conditions associated with the onset of ARDS lower the possibility of immediate ADSC retention in the lungs and complications, which may be associated with capillary occlusion by cells retained in the lungs. Abundant data in the literature show that the IV route of cell delivery renders preferential cell retention in the lungs immediately after injection<sup>10,11,13</sup>.

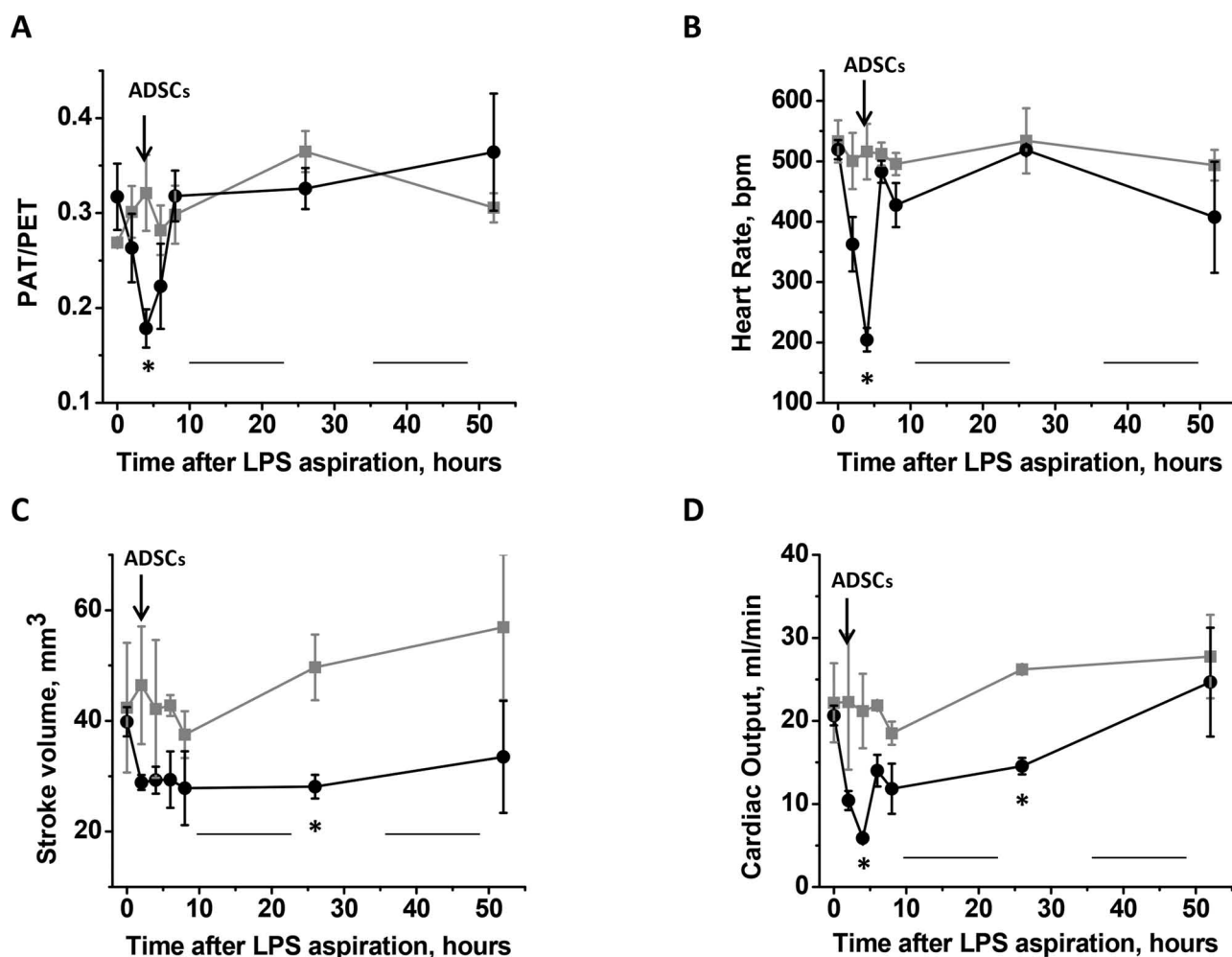


**Figure 4.** PAT/PET (A), heart rate (B), stroke volume (C), and cardiac output (D) for mice receiving saline (gray squares) or LPS (black circles) via oropharyngeal aspiration ( $n=3$  per group). Black lines indicate periods of dark (12-h light/dark cycle). First time point of the day was recorded at 8:00 a.m. Arrows indicate a point in time when adipose-derived stem cells (ADSCs) would be delivered. \* $p < 0.05$  between responses of control animals and animals exposed to LPS.

The objective of this study was to compare distribution of cells to naive and LPS-challenged lungs, as well as other internal organs including the brain. The information gained is quite critical for the development and optimization of ARDS therapy; it also offers insights for the physicians considering ADSC application for the inflammatory pathological conditions of the other organs.

We observed that approximately 10% to 15% of injected ADSCs were retained in healthy murine lungs 0–2 h after bolus delivery of 300,000 cells. This number was somewhat lower than previously reported in the literature<sup>11</sup>, although the number of cells per injection, the animal model, and the method of detection probably affected the outcome and analysis. Importantly, we observed that LPS-primed lungs retained approximately half the amount of ADSCs found in healthy lungs within the first 2 h after injection. To understand why the amount of cells retained in LPS-primed lungs is reduced, we assessed the effect of aspirated LPS on hemodynamics. Although data in the literature consistently link systemic delivery of LPS to an increase in pulmonary artery pressure<sup>18,19</sup>, studies on intratracheal administration of LPS are rather limited and show dependence of LPS-induced pulmonary hypertension on the presence of other triggers<sup>20</sup>. Keeping in mind that LPS administration to the lungs mimics ARDS caused by pneumonia rather than sepsis and therefore may have different effects than systemic LPS administration, we undertook the study of pulmonary hemodynamics following LPS aspiration. Our data demonstrate that LPS-challenged mice manifest significant reductions in PAT/PET ratios, indicative of an increase in pulmonary artery pressure<sup>16</sup>. LPS-challenged mice also manifest markedly reduced cardiac output 4 h post-LPS administration. All of these changes coincide with the peak of hypothermic shock<sup>17</sup>, which was used earlier to choose the point for therapeutic intervention. We are fully aware that these initial changes in hemodynamics reflect a direct reaction of the lungs to LPS rather than ARDS-related changes. However, cardiac output remains significantly decreased 24 h post-LPS challenge (Fig. 4), when ARDS is fully developed in this model<sup>17</sup>. We believe that significant reductions in cardiac output observed in our model make it clinically relevant to the changes in cardiac output observed in ARDS patients. Increased pulmonary vascular resistance in ARDS is often linked to elevated right ventricular afterload, which may produce right ventricular dysfunction and failure<sup>21,22</sup>. Not surprisingly, agents reducing pulmonary artery pressure, such as nitric oxide (NO), also increase cardiac output when acute right heart failure is present<sup>23,24</sup>, linking changes in cardiac output to both the severity of ARDS and the efficiency of therapeutic interventions.

While pulmonary vasoconstriction is likely to affect larger vessels and not have a substantial effect on the ability

of ADSCs to circulate freely, the decreased rate at which bolus-delivered ADSCs are perfused through the pulmonary capillary bed is likely to reduce the incidence of steric capillary occlusion by large particles such as ADSCs. Even though MSCs, whether bone marrow or adipose derived, are unlikely to be delivered to ARDS patients as a rapid bolus, current safety studies opt for IV delivery of ADSCs or bone marrow-derived MSCs (BM-MSCs). For instance, one study of ADSC transplantation for ARDS utilized a dose of  $10^6$  cells/kg delivered over a period of 1 h<sup>14</sup>. Another study of BM-MSC transplantation for ARDS (NCT01775774 at clinicaltrials.gov) utilized 1, 5, and  $10 \times 10^6$  cells/kg dose delivered over a period of 60–80 min<sup>25</sup>. For comparison, in our study,  $15 \times 10^6$  cells/kg rapid bolus delivery was tested. The fact that the reported safety study<sup>14</sup> suggested an increase in cell dosage in order to achieve a beneficial effect on ARDS calls for increased attention to the rate of cell delivery, which may increase cell retention in the lungs and the possibility of pulmonary bed occlusion. In light of the data presented here, pulmonary hypertension and the reduction of cardiac output in ARDS patients<sup>21,22</sup>, also observed in our model at the time of cell delivery, may reduce the risk of capillary occlusion due to steric blocking of the capillary bed with intravenously delivered cells.

Importantly, the dynamics of cell distribution change dramatically in the following 48 h. Twenty-four hours after ADSC administration, control lungs demonstrated marked reduction of ADSC levels, reaching negligible levels at 48 h. On the contrary, LPS-challenged lungs retained 6% and 3% of the delivered ADSC dose 24 and 48 h postinjection, respectively. These data are consistent with the data of others showing ~1% retention after 72 h<sup>26</sup>. Previously, we had shown a strong inflammatory response in LPS-challenged lungs 24 and 48 h post-LPS administration<sup>17</sup>. We speculate that the inflammation contributes to the sustained retention of ADSCs in ARDS-affected versus control lungs.

Dissimilar to the lung, other organs had only minor retention of ADSCs following IV delivery. These data suggest that when direct organ targeting is needed, cells have to be delivered locally rather than peripherally. On the other hand, an increase in mortality was shown when stem cells were delivered in the left atrium, possibly due to the embolism of cardiac circulation<sup>11</sup>. We failed to detect redistribution of ADSCs to the spleen or liver, as shown in other reports<sup>27</sup>. Possible redistribution to the thoracic lymph nodes<sup>28</sup> was not analyzed here.

A low percentage of stem cell engraftment in the lungs compared to the original delivered dose led others to speculate that the effect on ARDS is mostly paracrine<sup>26</sup>. That is, that the effects were mediated by the factors secreted by stem cells engrafted elsewhere. Although we cannot completely exclude this possibility, our data show that the time-dependent curves of ADSC distribution in other

organs follow the time-dependent curve of ADSC distribution in the lungs, with a higher cell level in the first 2 h following injection and a decrease in the following 48 h. Our data clearly show that ARDS-affected lungs are the only organs that harbor a substantial amount of ADSCs 48 h postinjection, making pulmonary-engrafted ADSCs the primary source of the therapeutic material.

In conclusion, we demonstrated that ARDS-affected lungs retain a reduced amount of IV-delivered ADSC bolus within the first 2 h after delivery. On the contrary, 48 h later only ARDS-affected lungs retain a substantial amount of ADSCs. No evidence of significant cell distribution to other organs at this time point was found in control mice or mice with ARDS. Our findings provide novel insights necessary for the development and optimization of cell-based therapy for ARDS.

*ACKNOWLEDGMENTS:* This work was supported by Krannert Institute of Cardiology Endowment Fund (N.V.B.), CTSI CECARE (N.V.B.), and Vascular and Cardiac Center for Adult Stem Cell Therapy and the Cryptic Masons Medical Research Foundation. The work was done with the use of facilities of Rousebush Veteran Affairs Medical Center. The authors are grateful to Dr. Dmitry Traktuev for the technical assistance with some of the experiments, and to Noelle Dahl for the help with manuscript preparation. There is a provisional patent filed by K.L.M. and N.V.B. for the treatment of ARDS with ADSC conditioned media.

## REFERENCES

- Ranieri VM, Rubenfeld GD, Thompson BT, Ferguson ND, Caldwell E, Fan E, Camporota L, Slutsky AS. Acute respiratory distress syndrome: The Berlin definition. *JAMA* 2012;307(23):2526–33.
- Fanelli V, Vlachou A, Ghannadian S, Simonetti U, Slutsky AS, Zhang H. Acute respiratory distress syndrome: New definition, current and future therapeutic options. *J Thorac Dis.* 2013;5(3):326–34.
- Boyle AJ, Sweeney RM, McAuley DF. Pharmacological treatments in ARDS; a state-of-the-art update. *BMC Med.* 2013;11(1):166.
- Fanelli V, Ranieri VM. Mechanisms and clinical consequences of acute lung injury. *Ann Am Thorac Soc.* 2015; 12(1 Suppl):S3–8.
- Walter J, Ware LB, Matthay MA. Mesenchymal stem cells: Mechanisms of potential therapeutic benefit in ARDS and sepsis. *Lancet Respir Med.* 2014;2(12):1016–26.
- Standiford TJ, Ward PA. Therapeutic targeting of acute lung injury and acute respiratory distress syndrome. *Transl Res.* 2016;167(1):183–91.
- Tatsumi K, Ohashi K, Matsubara Y, Kohori A, Ohno T, Kakidachi H, Horii A, Kanegae K, Utoh R, Iwata T, Okano T. Tissue factor triggers procoagulation in transplanted mesenchymal stem cells leading to thromboembolism. *Biochem Biophys Res Commun.* 2013;431(2):203–9.
- Tomashefski JF Jr, Davies P, Boggis C, Greene R, Zapol WM, Reid LM. The pulmonary vascular lesions of the adult respiratory distress syndrome. *Am J Pathol.* 1983;112(1):112–26.
- Idris NM, Li Z, Ye L, Sim EK, Mahendran R, Ho PC, Zhang Y. Tracking transplanted cells in live animal using upconversion fluorescent nanoparticles. *Biomaterials* 2009; 30(28):5104–13.
- Yukawa H, Watanabe M, Kaji N, Okamoto Y, Tokeshi M, Miyamoto Y, Noguchi H, Baba Y, Hayashi S. Monitoring transplanted adipose tissue-derived stem cells combined with heparin in the liver by fluorescence imaging using quantum dots. *Biomaterials* 2012;33(7):2177–86.
- Elhami E, Dietz B, Xiang B, Deng J, Wang F, Chi C, Goertzen AL, Mzengeza S, Freed D, Arora RC, Tian G. Assessment of three techniques for delivering stem cells to the heart using PET and MR imaging. *EJNMMI Res.* 2013;3(1):72.
- Forde A, Constien R, Grone HJ, Hammerling G, Arnold B. Temporal Cre-mediated recombination exclusively in endothelial cells using Tie2 regulatory elements. *Genesis* 2002; 33(4):191–7.
- Schrepfer S, Deuse T, Reichenspurner H, Fischbein MP, Robbins RC, Pelletier MP. Stem cell transplantation: The lung barrier. *Transplant Proc.* 2007;39(2):573–6.
- Zheng G, Huang L, Tong H, Shu Q, Hu Y, Ge M, Deng K, Zhang L, Zou B, Cheng B, Xu J. Treatment of acute respiratory distress syndrome with allogeneic adipose-derived mesenchymal stem cells: A randomized, placebo-controlled pilot study. *Respir Res.* 2014;15(1):39.
- Zhang S, Danchuk SD, Imhof KM, Semon JA, Scruggs BA, Bonvillain RW, Strong AL, Gimble JM, Betancourt AM, Sullivan DE, Bunnell BA. Comparison of the therapeutic effects of human and mouse adipose-derived stem cells in a murine model of lipopolysaccharide-induced acute lung injury. *Stem Cell Res Ther.* 2013;4(1):13.
- Thibault HB, Kurtz B, Raheer MJ, Shaik RS, Waxman A, Derumeaux G, Halpern EF, Bloch KD, Scherrer-Crosbie M. Noninvasive assessment of murine pulmonary arterial pressure: Validation and application to models of pulmonary hypertension. *Circ Cardiovasc Imaging* 2010;3(2):157–63.
- Lu H, Poirier C, Cook T, Traktuev DO, Merfeld-Claus S, Lease B, Petrache I, March KL, Bogatcheva NV. Conditioned media from adipose stromal cells limit lipopolysaccharide-induced lung injury, endothelial hyperpermeability and apoptosis. *J Transl Med.* 2015;13(1):67.
- Chlopicki S, Walski M, Bartus JB. Ultrastructure of immediate microvascular lung injury induced by bacterial endotoxin in the isolated, no-deficient lung perfused with full blood. *J Physiol Pharmacol.* 2005;56(4 Suppl):47–64.
- Kreil EA, Greene E, Fitzgibbon C, Robinson DR, Zapol WM. Effects of recombinant human tumor necrosis factor alpha, lymphotoxin, and Escherichia coli lipopolysaccharide on hemodynamics, lung microvascular permeability, and eicosanoid synthesis in anesthetized sheep. *Circ Res.* 1989;65(2):502–14.
- Lorenzoni AG, Wideman RF Jr. Intratracheal administration of bacterial lipopolysaccharide elicits pulmonary hypertension in broilers with primed airways. *Poult Sci.* 2008;87(4): 645–54.
- Price LC, McAuley DF, Marino PS, Finney SJ, Griffiths MJ, Wort SJ. Pathophysiology of pulmonary hypertension in acute lung injury. *Am J Physiol Lung Cell Mol Physiol.* 2012;302(9):L803–15.
- Ryan D, Frohlich S, McLoughlin P. Pulmonary vascular dysfunction in ARDS. *Ann Intensive Care* 2014;4:28.
- Benzing A, Mols G, Beyer U, Geiger K. Large increase in cardiac output in a patient with ARDS and acute right heart failure during inhalation of nitric oxide. *Acta Anaesthesiol Scand.* 1997;41(5):643–6.
- Puybasset L, Stewart T, Rouby JJ, Cluzel P, Mourgeon E, Belin MF, Arthaud M, Landault C, Viars P. Inhaled nitric oxide reverses the increase in pulmonary vascular

- resistance induced by permissive hypercapnia in patients with acute respiratory distress syndrome. *Anesthesiology* 1994;80(6):1254–67.
25. Wilson JG, Liu KD, Zhuo H, Caballero L, McMillan M, Fang X, Cosgrove K, Vojnik R, Calfee CS, Lee JW, Rogers AJ, Levitt J, Wiener-Kronish J, Bajwa EK, Leavitt A, McKenna D, Thompson BT, Matthay MA. Mesenchymal stem (stromal) cells for treatment of ARDS: A phase 1 clinical trial. *Lancet Respir Med*. 2015;3(1):24–32.
  26. Chien MH, Bien MY, Ku CC, Chang YC, Pao HY, Yang YL, Hsiao M, Chen CL, Ho JH. Systemic human orbital fat-derived stem/stromal cell transplantation ameliorates acute inflammation in lipopolysaccharide-induced acute lung injury. *Crit Care Med*. 2012;40(4):1245–53.
  27. Wang N, Shao Y, Mei Y, Zhang L, Li Q, Li D, Shi S, Hong Q, Lin H, Chen X. Novel mechanism for mesenchymal stem cells in attenuating peritoneal adhesion: Accumulating in the lung and secreting tumor necrosis factor alpha-stimulating gene-6. *Stem Cell Res Ther*. 2012;3(6):51.
  28. Islam MN, Das SR, Emin MT, Wei M, Sun L, Westphalen K, Rowlands DJ, Quadri SK, Bhattacharya S, Bhattacharya J. Mitochondrial transfer from bone-marrow-derived stromal cells to pulmonary alveoli protects against acute lung injury. *Nat Med*. 2012;18(5):759–65.